

Electronic Supplementary Information for

## Chelate-induced formation of $\text{Li}_2\text{MnSiO}_4$ nanorods as a high-capacity cathode material for Li-ion batteries

Yi Pei,<sup>a, b, c, #</sup> Qing Chen,<sup>a, b, #</sup> Cheng-Yan Xu,<sup>a, b, \*</sup> Hui-Xin Wang,<sup>a</sup> Hai-Tao Fang,<sup>a</sup>  
Chang Zhou,<sup>a</sup> Liang Zhen,<sup>a, b, \*</sup> Guozhong Cao<sup>c, \*</sup>

<sup>a</sup> School of Materials Science and Engineering, Harbin Institute of Technology, Harbin 150001, China

<sup>b</sup> MOE Key Laboratory of Micro-systems and Micro-structures Manufacturing, Harbin Institute of Technology, Harbin 150080, China

<sup>c</sup> Department of Materials and Engineering, University of Washington, Seattle, WA 98195-2120, USA

<sup>#</sup> These authors contributed equally to this work.

<sup>\*</sup> Corresponding authors. E-mail: cy\_xu@hit.edu.cn (C.Y. Xu); lzhen@hit.edu.cn (L. Zhen); gzcao@u.washington.edu (G. Cao)

### Computation methods

DFT calculations were performed using a plane wave basis set with the projector augmented wave framework<sup>1</sup> describing the core electrons. The exchange-correlation energy was evaluated within generalized gradient approximation with a Hubbard U correction.<sup>2</sup> An effective U value of 4 eV was used for the d-states of the transition metals. An energy cutoff for the plane wave basis was set at 520 eV. Integration in the Brillouin zone was done with a 6×6×6 Monkhorst-Pack k-point mesh. Structural optimization was continued until the force on each atom reached 0.01 eV/Å. All structures were relaxed in terms of both cell parameters and atomic positions. Li diffusion barriers in half-delithiated state were calculated in a 2×2×2 supercell using nudged elastic band method.

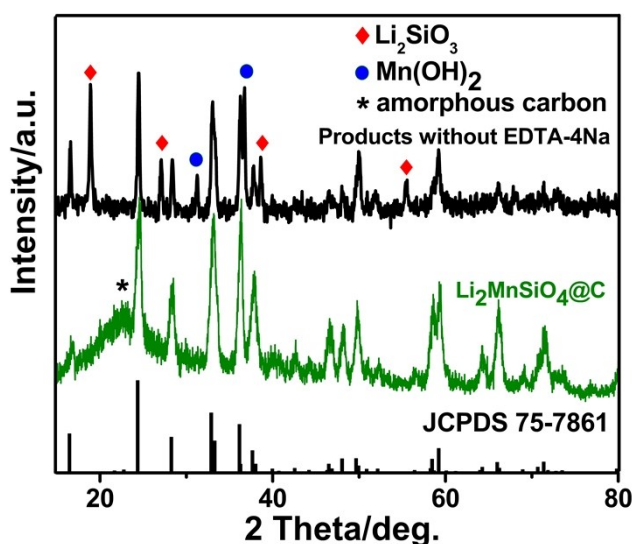


Fig. S1 XRD pattern of products without EDTA-4Na and  $\text{Li}_2\text{MnSiO}_4$ @C.

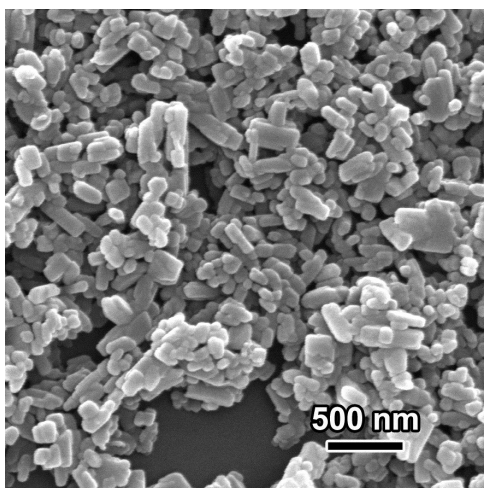


Fig. S2 SEM image of products without EDTA-4Na.

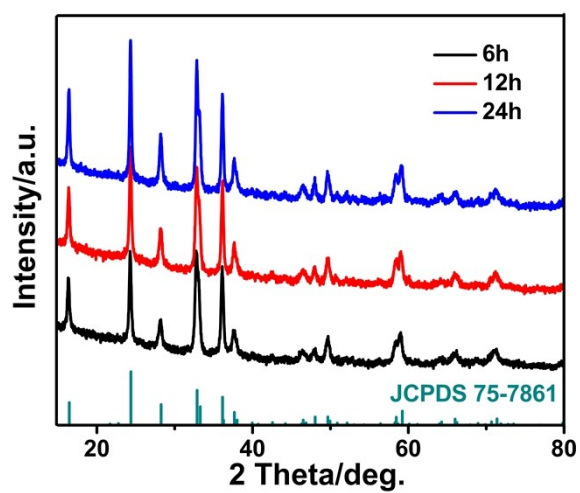
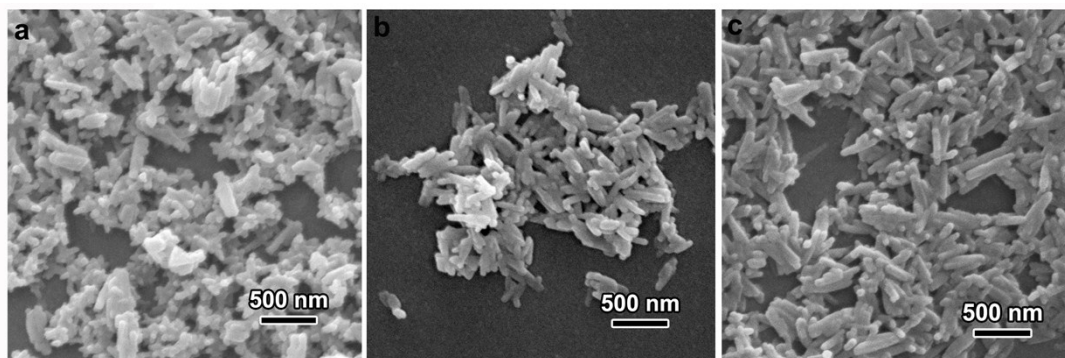
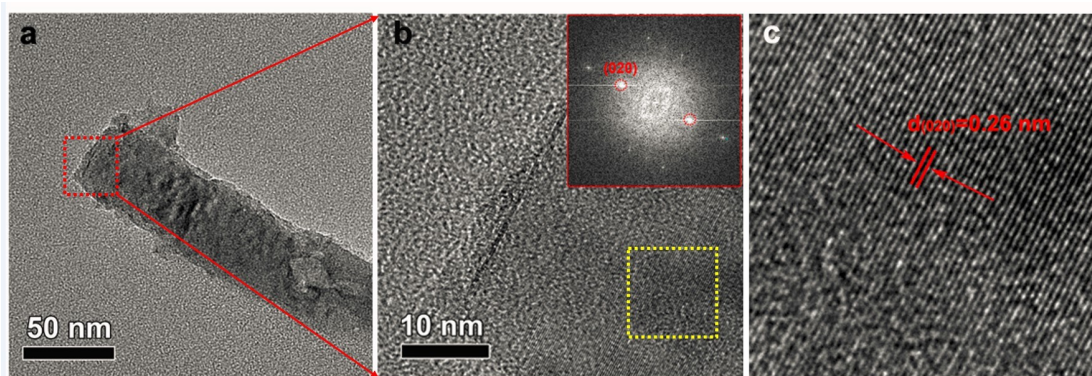


Fig. S3 XRD pattern of  $\text{Li}_2\text{MnSiO}_4$  samples synthesized with different reaction durations. XRD patterns indicated that all the samples are phase-pure  $\text{Li}_2\text{MnSiO}_4$ , and the sample crystallinity increases slightly with prolonging reaction time.



**Fig. S4** SEM images of  $\text{Li}_2\text{MnSiO}_4$  samples synthesized with different reaction durations: (a) 6h; (b) 12h; (c) 24h. With a short reaction duration of 6h, a few  $\text{Li}_2\text{MnSiO}_4$  nanorods were formed accompanied with nanoparticles, as shown in Fig. S4(a). Increasing the reaction duration leads to the yield of nanorods without changing the diameters (see Fig. S4(b) and (c)).



**Fig. S5** (a) Low-magnification TEM image of an individual  $\text{Li}_2\text{MnSiO}_4$  nanorod. (b) HRTEM image of the tip of rod (red square in (a)). Inset is FFT pattern. (c) Enlarged HRTEM image showing well-resolved (020) interplanar distance. Fig. S5(a) was a low-magnification TEM image of an individual  $\text{Li}_2\text{MnSiO}_4$  nanorod, and its HRTEM image (lattice fringes not resolved due to small image size) was shown in Fig. S5(b). Inset in Fig. S5(b) is fast Fourier transformation (FFT) pattern of the labelled area, and enlarged HRTEM image of the same area showing well-resolved (020) lattice fringes was given in Fig. S5(c). It was obviously that (020) facet is parallel to the ending plane of  $\text{Li}_2\text{MnSiO}_4$  nanorods, and thus the preferential growth direction of  $\text{Li}_2\text{MnSiO}_4$  nanorods is its [010] crystallographic direction, which is consistent with previous report<sup>3</sup>.

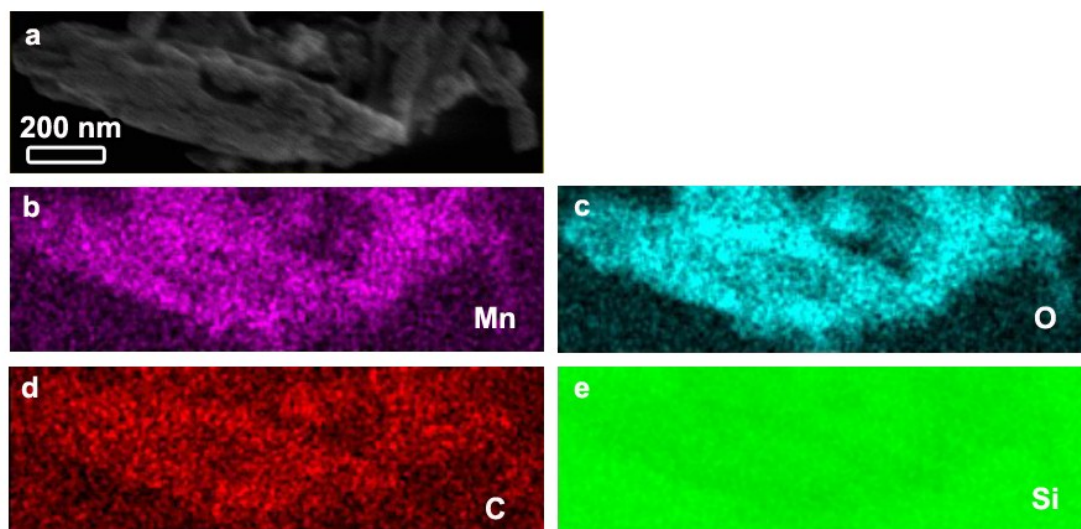


**Fig. S6** (a) SEM image and the specifically resolved (b) Mn; (c) O; (d) C and (e) Si elemental mapping of the sample.

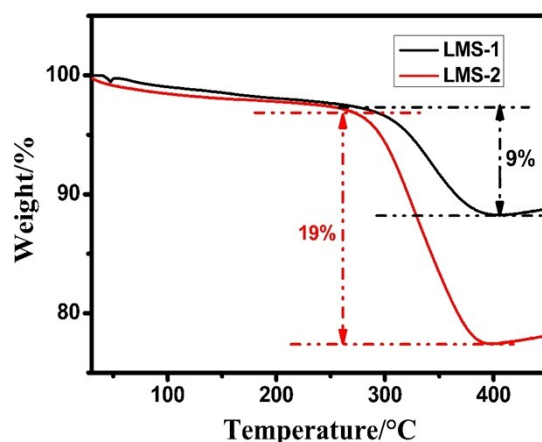


**Fig. S7** TG curves of  $\text{Li}_2\text{MnSiO}_4@\text{C}$  with different amounts of carbon coating.

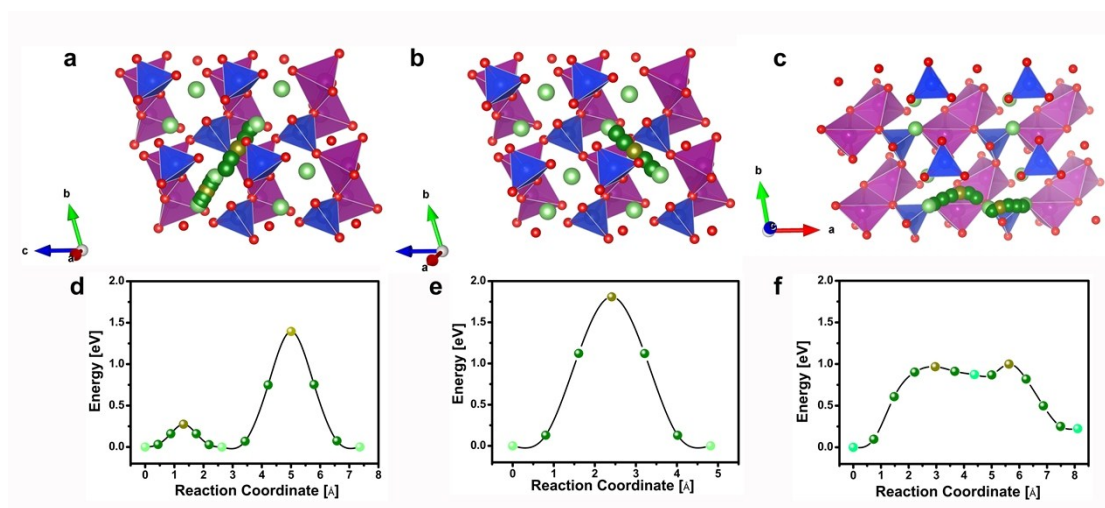


**Fig. S8** (a, b, c) Three probable Li ion diffusion paths in half-lithiated state ( $\text{LiMnSiO}_4$ ) and (d, e, f) the corresponding migration barriers. Light green, dark green and brown denote end-, intermediate-, and saddle-points, respectively. According to DFT calculations, Islam et al. pointed out that the [001] or [100] direction are the major migration pathways for Li ions in  $\text{Li}_2\text{MnSiO}_4$  with orthorhombic  $Pmn2_1$  structure<sup>4</sup>. The obtained  $\text{Li}_2\text{MnSiO}_4$  nanorods in this work grow along the [010] crystallographic direction, and thus the migration pathways along [001] or [100] direction are short for Li ions, which is benefit for enhanced electrochemical performance. Moreover, in our parallel DFT theoretic investigation of  $\text{Li}_2\text{MnSiO}_4$ <sup>5</sup>, it was found that when half of the total Li ions were extracted from the host, the material will undergo a notable phase transition to a collapsed framework by connecting two tetrahedra from the neighboring layers to form edge sharing  $\text{MnO}_5$  square pyramids. Li ion diffusion ability in collapsed  $\text{LiMnSiO}_4$  should be different from that in layered  $\text{Li}_2\text{MnSiO}_4$ . Accordingly, Li diffusion barrier in collapsed  $\text{LiMnSiO}_4$  was calculated and compared in Fig. S8. Three probable Li ion diffusion paths in collapsed  $\text{LiMnSiO}_4$  and the corresponding migration barriers

were presented. Light green, dark green and brown in the picture denoted end-, intermediate-, and saddle-points, respectively. The migration activation energy in path a, b, c are calculated to be 1.5, 1.8 and 0.97 eV, respectively, suggesting the diffusion of Li prefers to be along [100] direction in collapsed LiMnSiO<sub>4</sub>. Thus, the one-dimensional morphology of LiMnSiO<sub>4</sub> nanorods with short migration distances along the [100] and [001] directions should benefit the Li<sup>+</sup> diffusion at both full and half-lithiated state of Li<sub>2</sub>MnSiO<sub>4</sub>.

#### References:

- 1 P. E. Blöchl, *Phys. Rev. B* 1994, **50**, 17953.
- 2 A. I. Liechtenstein, V. I. Anisimov, J. Zaanen, *Phys. Rev. B* 1995, **52**, R5467.
- 3 H. J. Song, J. Kim, M. Choi, C. Choi, M. A. Dar, C. W. Lee, S. Park and D. Kim, *Electrochim Acta*, 2015, **180**, 756.
- 4 C. A. J. Fisher, N. Kuganathan and M. S. Islam, *J Mater Chem A*, 2013, **1**, 4207.
- 5 Q. Chen, P. H. Xiao, Y. Pei, Y. Song, C. Y. Xu, L. Zhen, G. Henkelman, *Chem Mater*. 2016, Submitted.